



**Please cite the Published Version**

Crapnell, Robert D  and Banks, Craig E  (2024) Electroanalysis overview: the determination of the poisoner's poison, thallium. *Talanta Open*, 9. 100291 ISSN 2666-8319

**DOI:** <https://doi.org/10.1016/j.talo.2024.100291>

**Publisher:** Elsevier BV

**Version:** Published Version

**Downloaded from:** <https://e-space.mmu.ac.uk/633923/>

**Usage rights:**  [Creative Commons: Attribution-Noncommercial-No Derivative Works 4.0](#)

**Additional Information:** This is an open access article which originally appeared in *Talanta Open*

**Data Access Statement:** No data was used for the research described in the article.

**Enquiries:**

If you have questions about this document, contact [openresearch@mmu.ac.uk](mailto:openresearch@mmu.ac.uk). Please include the URL of the record in e-space. If you believe that your, or a third party's rights have been compromised through this document please see our Take Down policy (available from <https://www.mmu.ac.uk/library/using-the-library/policies-and-guidelines>)



# Electroanalysis overview: The determination of the poisoner's poison, thallium

Robert D. Crapnell, Craig E. Banks\*

Faculty of Science and Engineering, Manchester Metropolitan University, Chester Street, Manchester M1 5GD, United Kingdom

## ARTICLE INFO

### Keywords:

Electroanalysis  
Thallium  
Sensors  
Electrochemistry

## ABSTRACT

In this overview, we explore the electroanalytical determination of the poisoner's poison: thallium. Thallium was named after the Greek word "thallos," meaning "green shoot" or "twig," due to its bright green spectral emission lines. It is toxic, tasteless, odourless and dissolves into water, and has been used by murderers as a challenging poison to detect and there is the need for the analytical determination of thallium. Laboratory based analytical instrumentation provide a routine methodology to measure thallium, but there is scope to develop in-the-field analytical measurements that are comparable to laboratory equipment and in some cases, they can provide even more sensitive analytical approaches. Electrochemistry can support such endeavours, where instrumentation are readily portable where electroanalytical sensors provide highly selective and sensitive outputs but yet are economical to support on-site analysis. In this review, we provide an electroanalytical overview of the current research directed toward the measurement of thallium and offer insights to future research.

## 1. Introduction to thallium

Thallium is known as the *poisoner's poison* due to its sinister properties that make it an effective position in a plethora of criminal activities. Thallium was discovered by Sir William Crookes around 1861 and it is named after the Greek word "thallos," meaning "green shoot" or "twig," due to its bright green spectral emission lines. [1] Thallium is toxic, tasteless, odourless and dissolves into water, giving it ideal properties to be used by murderers as it is difficult to detect. In the early 1800s, thallium sulphate was used to treat medical conditions such as gout, gonorrhoea, and syphilis, but with its side effects, it was not widely used. Thallium sulphate has a history of being used as a rodenticide and insecticide, but many countries banned its use around 1970s due to unintentional or criminal poisonings of humans. Thallium poisoning may include vomiting and nausea, skin hyperaesthesia mainly in the soles of the feet and the tibia, alopecia, Mee's lines on nails, fever, gastrointestinal problems, delirium, convulsions and comas [2–9]. The most characteristic sign of thallium toxicity is alopecia which usually appears in cases when death is delayed for 15–20 days [10–15]. The reason for thallium's high toxicity is that the thallium (I) ion has similarities with the essential alkali metal cations, particularly with potassium due to similar ionic radii ( $Tl^+$ : 164 pm,  $K^+$ : 152 pm) and thus it enters the body via potassium uptake pathway [16]. The lethal thallium

dose in humans is reported to be 10–15 mg/kg; but deaths can occur in adults with doses as low as 8 mg/kg [17]. Thallium has two principal oxidation states, thallium (I) and thallium (III), both of which are considered highly toxic to living organisms, where thallium (I) is expected to be the dominant species in aqueous solution at equilibrium with atmospheric oxygen and in the absence of complexing agents [16, 18]. We note that U.S. Environmental Protection Agency maximum contaminant level for thallium in drinking water is  $2 \mu\text{g L}^{-1}$  (0.098  $\mu\text{M}$ /98 nM) [19,20].

There are many infamous criminals who used thallium as a poison (thallotoxicosis), such as: the *Teacup Poisoner*, Graham Young, who killed 3 victims over 1962–1971 by spiking thallium into the food and drink of relatives and school friends; the *Mensa Murderer*, George Trepal, a chemist, computer programmer and a former member of Mensa with an I.Q. of 130+, killed his neighbour by adding thallium to multiple bottles of Coca-Cola®, and was subsequently sentenced to death by electrocution in 1991 [21,22]. Other reports of a 23-year-old woman (2017) who was poisoned by a business colleague when she unknowingly drank tea at school and noticed that the taste was different from ordinary tea [17]; the woman was treated with multi-dose activated charcoal with airway protection and Prussian blue – which is the current therapy for thallium poisoning [23]. There is a longlist of thallium poisonings, and as writing this article, end of 2023, there are still today

\* Corresponding author.

E-mail address: [c.banks@mmu.ac.uk](mailto:c.banks@mmu.ac.uk) (C.E. Banks).

<https://doi.org/10.1016/j.talo.2024.100291>

Received 9 December 2023; Received in revised form 10 January 2024; Accepted 23 January 2024

Available online 29 January 2024

2666-8319/© 2024 The Authors. Published by Elsevier B.V. This is an open access article under the CC BY-NC-ND license (<http://creativecommons.org/licenses/by-nc-nd/4.0/>).

the use of using thallium in poisonings, such as reported in India and Japan [24,25].

Despite the criminal activities, thallotoxicosis, thallium is in the environment due to anthropogenic activities such as cement production, burning of fossil fuel, petroleum refining and exhaust emissions, use in the electricals and the electronics industry, and medical procedures which can lead to the deposition of thallium in water and soils, contaminating rivers and leading to contaminated foods [26,27].

Consequently, there is the need for the detection of thallium which has been reported using flame atomic absorption spectrometry (FAAS) [28], inductively coupled plasma mass spectrometry (ICP-MS) [29], spectrofluorimetric [30], inductively coupled plasma optical emission spectrometry (ICP-OES) [31], and solid sampling high-resolution continuum source graphite furnace atomic absorption spectrometry (SS HR-CS GF AAS) [32]. Note that the low concentration of thallium in water samples necessitates analysis methods with high sensitivity and low detection

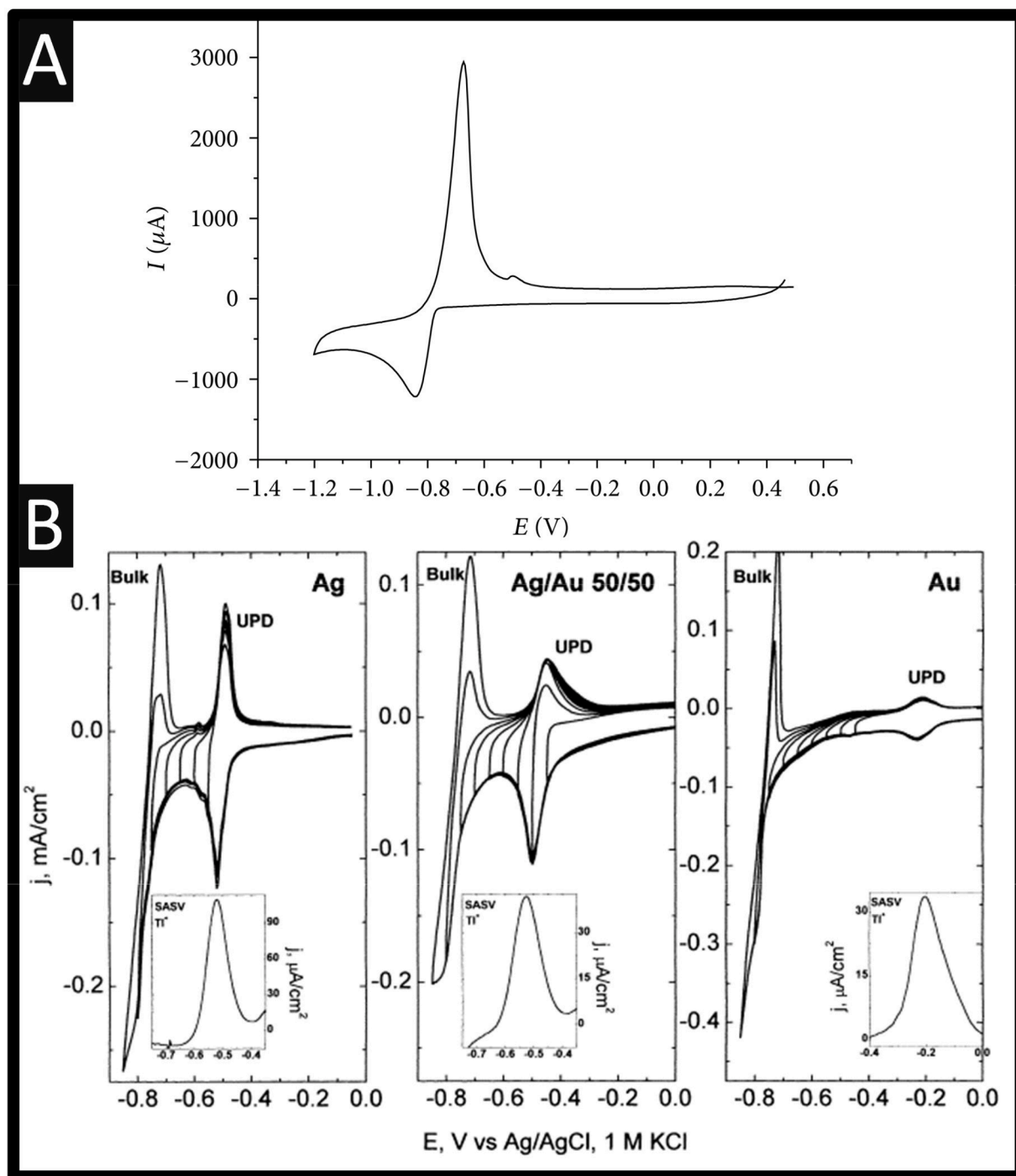


**Fig. 1.** A Cyclic voltammogram of thallium obtained using a glassy carbon electrode; Conditions: 1 mM thallium; electrolyte: pH 7; Scan rate:  $20 \text{ mVs}^{-1}$ . Figure reproduced from reference [45]. Copyright Hindawi Publishing Corporation B: Cyclic voltammograms recorded using a silver, gold and a silver-gold alloy macroelectrodes towards the detection of thallium. Solution: 0.5 mM thallium, 10 mM nitric acid and 10 mM sodium chloride. Scan rate:  $25 \text{ mVs}^{-1}$ . The insert shows the use of substrate anodic stripping voltammetry (SASV) of 300 nM thallium. Conditions of electrodeposition:  $E_{\text{dep}} = -0.7 \text{ V}$  for silver and the silver-gold alloys and  $-0.4 \text{ V}$  for gold;  $t_{\text{dep}}$ : 30 s; rotating rate, 3500 rpm. SW mode: square-wave amplitude, 10 mV; step amplitude, 2.5 mV; frequency, 25 Hz. Figure reproduced from reference ([40]). Copyright 2003 Wiley.

limits, which often require a separation and preconcentration step(s) of thallium such as liquid-liquid, solid-phase and cloud point extractions [33–35]. These instruments provide analytical techniques with high selectivity and sensitivity, but have drawbacks, including tedious sample preparation, the requirement for highly skilled operators, high operational costs, and lengthy analysis time involving pre-concentration step(s), calibration, preparation, and sampling [36]. There is a need for simple and inexpensive instrumentation that gives highly accurate and sensitive analytical results and allows in-the-field measurements. An alternative approach that can achieve this is the use of electroanalysis, which is a powerful tool for quantitative chemical analysis and finds applications in a wide range of fields allowing for real-time monitoring and precise measurements. This makes it valuable in both research and practical applications such as in pH sensors, glucose sensors, and electrochemical biosensors for medical and environmental monitoring. Electroanalytical methods have access to potentiostats that are hand-held, battery operated, and can be controlled by mobile devices via Bluetooth. Therefore, electrochemical sensing platforms have the benefits of being portable, low cost, rapid analysis times but yet are highly sensitive and selective towards the analyte being measured through the intelligent design of the sensing platforms.

## 2. Introduction to electroanalytical sensing of thallium

Thallium has two principal oxidation states,  $Tl^+$  and  $Tl^{+3}$ , however the focus is on the detection of thallium (I) and there are limited reports for the measurement of thallium (III). Throughout we refer to thallium, meaning thallium (I) as this is the prominent species being identified and in the case of thallium (III), we make it implicit. The issue of thallium (I) vs. thallium (III) resides in the fact that compounds of thallium (I) are water soluble, apart from the sulfide, whereas the solubility of compounds of thallium (III) are very low and dependant on pH [37]. The electroanalytical sensing of thallium uses the most sensitive electrochemical approach, anodic stripping voltammetry, whose outstanding sensitivity is attributed to the effective preconcentration step (and suitable reductive potential), but generally it is good practice to run a cyclic voltammetric experiment to see where the deposition and stripping of thallium occur upon your electrode surface. For example, as shown within Fig. 1A, we can observe the response of thallium using a glassy carbon electrode (GCE) where a single cathodic deposition signal is observed where this process is summarised [38–40]:



when the potential is reserved, the anode stripping signal can be seen which corresponds to:



where (m) indicated the electrode surface. This is repeated using silver, gold and a silver-gold alloy which shows the process observed within Fig. 1A but includes underpotential deposition; see Fig. 1B [40]. Note that the underpotential deposition (UPD) is defined as a metal monolayer that is electrodeposited on a foreign metal substrate at significantly less negative potentials than that for electrodeposition on the same metal; [41,42] UPD deposits usually involve sub-monolayers and monolayers. Ultimately, UPD is the result of attractive interactions between the depositing metal ions (thallium) and the metal substrate (e.g., silver), being stronger than the atomic interaction compared to the depositing metal upon other deposited metal(s). As a result of these interactions, a metal is deposited in the UPD region as a monolayer. Other work has explored the UPD on silver nanoparticles where they have been shown that it is size dependence, where it is absent for silver nanoparticles which are smaller than 50 nm in diameter, arising from size-dependant morphology or electronic (work function) properties [43]. Both the adsorption and stripping processes can be affected by the presence of adsorbed anions which can affect the observed peak

potential of either or both steps [44].

As observed from Fig. 1B, this offers two processes to which thallium can be measured, i.e., bulk vs. UPD, where the UPD process is exemplified by the insert subtractive anodic stripping voltammetry (SASV) where the potential is held at just past the cathodic reductive peak of UPD which gives rise to a sensitive response. The electroanalytical advantages of UPD over that of the bulk detection have been elegantly summarised by Herzog and Arrigan [41], where they state that in the case of UPD, low concentrations of metal are being deposited, the metallic deposit covers a very low portion of the working electrode surface and as such, the structure of the electrode surface remains mainly unchanged, resulting in a good repeatability of the analytical response. This obviously negates the need for polishing and electrochemical treatment of the electrode surface between experiments since there are a limited number of atoms being deposited (one monolayer maximum) on the electrode surface, the preconcentration step required is often short resulting in a rapid electroanalytical response. While the use of UPD for the electroanalytical sensing has benefits, which has been extensively applied to other metals [41], there are scarcely any reports using this for thallium [46] but mostly these are fundamental [44, 47–50].

We have summarised all electroanalytical reports reported for the determination of thallium within Table 1, which we can observe are diverse, ranging from mercury, bismuth, multi-walled carbon nanotubes, graphene and other variants that provide the sensing of thallium. As described above, the detection of thallium is achieved through anodic stripping voltammetry, which can be divided into square-wave anodic stripping voltammetry (SWASV) and differential pulse anodic stripping voltammetry (DPASV) that offer enhanced sensitivity compared to traditional voltammetry (e.g. linear sweep voltammetry) methods where the choice between the two depends on the specific analytical requirements, peak resolution, the nature of the electrochemical system, and the concentration range of interest. There are other approaches that can be used where we point these out. We present each case reported for the sensing of thallium through the following headings, where we start with mercury electrodes.

### 2.1. Mercury electrodes

Mercury electrodes, either film or hanging drop for example, have been the choice for the electroanalysis of metal ions, where it is useful for the sensing of thallium as it is highly soluble (43.0 at%). [51] Mercury electrodes enable negative potential to  $\sim -2.5$  V (vs. SCE) but the positive potential is limited to  $\sim +0.4$  V (vs. SCE). [52] Mercury electrodes have a high hydrogen overvoltage and the ability to form amalgams with metals, and due to the renewal of the mercury surface (relative to mercury drop electrode) alleviate the electrode passivation. However, the biggest drawback is its high toxicity and they have been restricted [52,53]. That said, we start overviewing the past history of the use of mercury for the detection of thallium. Let's consider the cyclic voltammogram obtained using a GCE electrode compared with a Nafion® mercury film GCE, as shown within Fig. 2A, which shows the characteristic peaks for the deposition of thallium (I) to thallium metal, forming an amalgamation, and the anodic stripping peak corresponding to the transition of thallium metal back to thallium (I) [54]. The authors noted that on the GCE the peak potential separation is wide, indicative of a quasi-reversible electrochemical reaction but in the case of mercury, these are more symmetric in shape indicating that the mercury electrode is more suitable for the detection of thallium [54]. Note the authors use of ethylenediaminetetraacetate (EDTA), which is added in order to reduce the large concentrations of interfering metal ions. This is a common theme that is repeated throughout the measurement of thallium with concentrations of EDTA has ranged from  $10^{-4}$  M to  $10^{-2}$  M [55–57]. Within Fig. 2B, we can observe the use of a bare GCE, a Nafion® film coated GCE, a mercury film coated GCE and the largest signal is observed using a Nafion® - mercury film GCE towards sensing

**Table 1**

An overview of recent approaches for the measurement of thallium.

Electrode	Modification	Linear Range	Limit of Detection	Sample Medium	Comments	Refs.
GCE	Nafion® -mercury film	244 pM–489 nM	48 pM	Tap, rain and ground water	–	[54]
GCE	poly(4-vinylpyridine) mercury film	4.9–489 nM	313 pM	Ground and lake water	Thallium (III); of potentiometric stripping analysis	[60]
GCE	poly(4-vinylpyridine) mercury film	9.7–49 nM	357 pM	Ground water and electroplating waste solution	Thallium (III); SWASV	[61]
GCE	Mercury film	1–500 nM	0.5 nM	Natural waters	–	[58]
GCE	Mercury film	down to 100 nM	2 nM	River water	Potentiometric stripping analysis	[62]
GCE	Mercury film	97–684 pM	–	Human urine	–	[112]
HMDE	–	1–4.8 µM	636 nM	Lake water	–	[113]
HMDE	DTPA	–	9.7 nM	Sewage water, horseradish	Compared with ICP-MS	[59]
HMDE	EDTA	10–500 µM	1 µM	–	–	[114]
HMDE	EDTA	11–97 nM	9.7 nM	Soil	In the presence of lead and copper	[63]
GCE	Mercury film	–	–	Soil and compost	Compared with AAS	[115]
CPE	Chitosan – mercury nanodroplets	4.8 nM–1.9 µM	978 pM	Tap, well and wastewater, human hair, certified reference material	–	[64]
GCE	Bismuth film	12–150 nM	10.8 nM	River water and Soil sample	–	[72]
GCE	Bismuth film	0.5–120 nM	2 nM	Berry juice	Simultaneous determination of thallium, lead and zinc	[77]
Bi nanopowder electrode	–	4.8 nM–2.4 µM	146 pM	NA	–	[75]
car-bon-epoxy composite electrode	Bismuth film	48 nM–4.8 µM	4.8 nM	Lithium carbonate	–	[73]
Bismuth bulk annular band electrode	–	48 pM–489 nM	4.8 pM	Tap, river water and a certified reference waters	–	[74]
SPE	Bismuth precursor	0–244 nM	4.4 nM	Certified lake water	–	[76]
SPE	Bismuth film	5 nM–1 µM	0.84 nM	Certified surface, natural and rainwater	–	[116]
CPE	Antimony film	48–489 nM	6.8 nM	–	–	[81]
GCE	Antimony film	97–489 nM	9.7 nM	Tap and river water	–	[82]
SPCNFE	4-carboxybenzo-18-crown-6	47–976 nM	–	Tap water	Simultaneous determination of thallium and indium; Compared to ICP-MS	[83]
ITO	ATT: MWCNTs	48–489 nM	6.3 nM	Industrial water	–	[86]
GCE	SnO <sub>2</sub> - MWCNTs	14 pM–2.2 µM	4.4 pM	River water	Simultaneous determination of mercury and thallium and compared with ICP-MS	[87]
CPE	IP-MWCNT	14 nM–1.1 µM	3.7 pM	Tap, well and wastewater and human hair	–	[88]
CPE	RTIL-L-MWCNTs	1.4 –342 nM	391 pM	Tap, lake and river water	–	[89]
GCE	Bi NPs- MWCNTs-PDA	1.9 nM–1.9 µM	195 pM	Mineral, tap and wastewater	Simultaneous determination of thallium and lead	[90]
SPCE	Bi film - MWCNTs	0.01–1 µM	2.8 nM	River water	–	[91]
GCE	MnO <sub>2</sub> @Fe <sub>3</sub> O <sub>4</sub> -Sep - MWCNT	489 pM–7.3 µM	146 pM	Tap, pool, well water and soil	Compared to ICP-OES	[93]
CPE	OPFP-L <sub>2</sub> -graphene	1.25–200 nM	0.35 nM	Tap, river water and soil	Simultaneous determination of thallium, lead and mercury and compared to GF-AAS	[92]
GCE	Graphene	9.78–97.8 nM	6 nM	Flour and grain products	–	[97]
Graphite fibre electrode	–	24 µM–1.7 µM	48 pM	River and groundwater	–	[117]
CPE	Prussian Blue	1–20 µM	–	Ground, Waste and Lake water	–	[102]
CPE	Amberlite LA-2	4.8–489 µM	97 µM	Fly ash	–	[101]
CPE	8-Hydroxyquinoline	0.5 nM–16 µM	0.23 nM	US EPA water pollution quality control sample, seawater and human urine.	Thallium (III)	[106]
CPE	8-Hydroxyquinoline	10 nM–10 µM	4.9 nM	US EPA water pollution quality control sample	–	[105]
GCE	Langmuir–Blodgett film of <i>p</i> -allylcalix[4]arene	24 nM–1.2 µM	4.8 nM	Tap and lake water	–	[103]
GCE	Langmuir – Blodgett (LB) film of a <i>p</i> -tert-butylcalix[4]arene	30 nM–4 µM	20 nM	Tap and lake water	Simultaneous determination of thallium and lead	[104]
GCE	Ag NPs-dextrin	50 nM–0.5 µM	35 nM	–	–	[98]
GCE	Iridium Oxide	4.8–99 µM	0.5 µM	–	–	[99]
GCE	Glycine	2 nM–0.2 µM	0.175 nM	Drinking, spring, river water and industrial wastewater	Simultaneous detection of thallium and mercury	[100]
GCE	Ag NPs-LS/Hg	12.2 nM–0.11 µM	4.6 nM	Soil	–	[108]

(continued on next page)

Table 1 (continued)

Electrode	Modification	Linear Range	Limit of Detection	Sample Medium	Comments	Refs.
GCE	Au NPs-LS/Hg	0.17–5 $\mu\text{M}$	0.14 $\mu\text{M}$	Soil		[110]
CPE	Crown ether (dicyclohexyl-18-crown-6)	14–1.2 $\mu\text{M}$	4.2 $\mu\text{M}$	Tap, well and wastewater and hair samples and certified reference material	–	[107]
CPE	ZIF-67 nanocrystals	0.1 nM–0.5 $\mu\text{M}$	0.01 nM	River water, soil and human urine and human hair	Compared to FAAS.	[111]

**Key:** MWCNTs: multi-walled carbon nanotubes; ATT: 3-Amino-1,2,4-triazole-5-thiol; RTIL: room temperature ionic liquid; L: noncyclic crown-type polyethers; GCE: glassy carbon electrode; CPE: carbon paste electrode; PDA: polydopamine; SPCE: screen-printed carbon electrodes; IP: imprinted polymer; OPFP: 1-n-octylpyridinium hexafluorophosphate; L<sub>2</sub>: [2,4-Cl<sub>2</sub>C<sub>6</sub>H<sub>3</sub>C(O)CHPh<sub>3</sub>]; Sep: magnetic sepiolite; HMDE: hanging mercury drop electrode; DTPA: diethylenetriaminepentaacetic acid; SPCNFE: screen-printed carbon nanofiber-modified electrode; Ag NPs: gold nanoparticles; LS: lignosulfonic acid derivative.

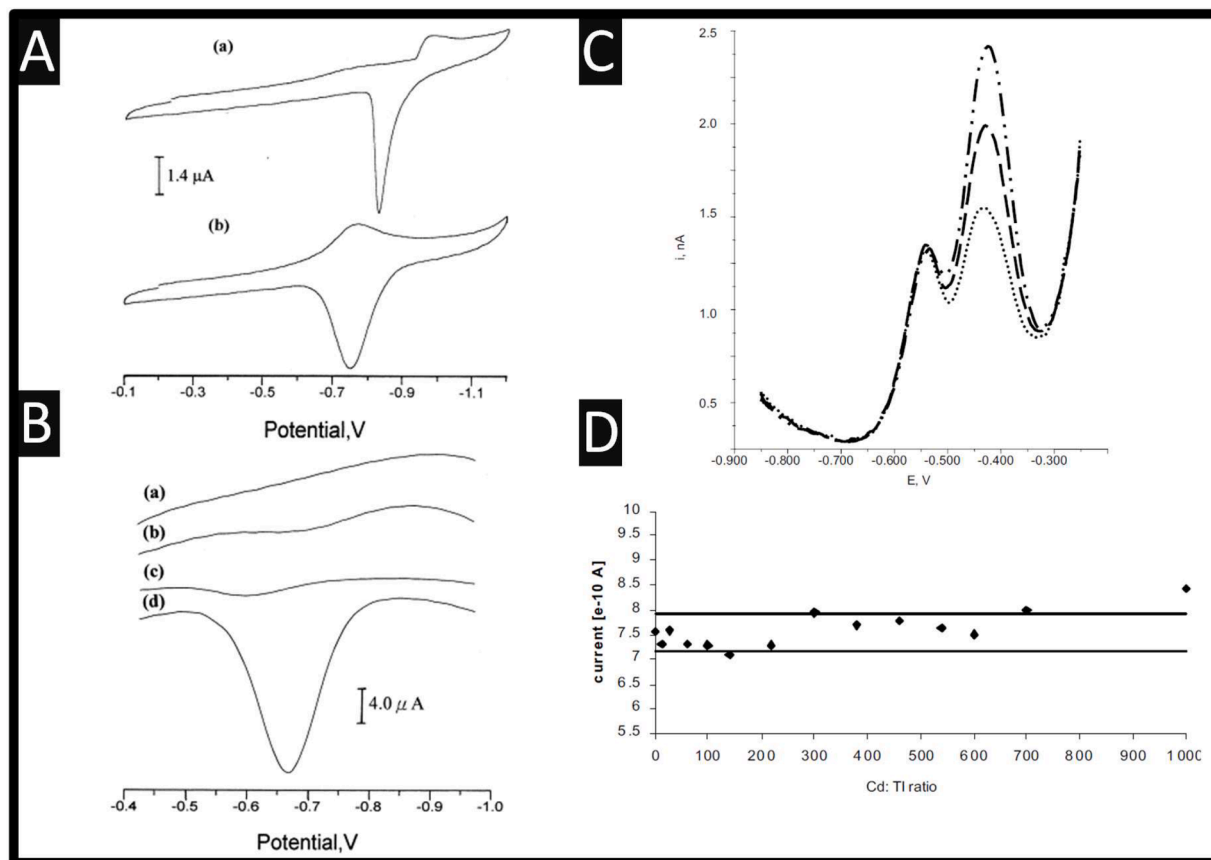


**Fig. 2.** A: An overview of cyclic voltammograms at a GCE (a), at the Nafion® - mercury film electrode. Conditions: thallium 4.8  $\mu\text{M}$  with 0.1 M NaNO<sub>3</sub> and 0.01 M EDTA. Potential is scanned from  $-0.2$  to  $1.2$  V and reversed to  $-0.1$  V (vs. Ag/AgCl). Scan rate:  $100 \text{ mV s}^{-1}$ . B: SWASV for 49  $\mu\text{M}$  thallium with 0.1 M NaNO<sub>3</sub> and 0.01 M EDTA (pH = 4.5) solution comparing: (a) bare GCE, (b) Nafion® film coated GCE, (c) mercury film coated GCE and (d) Nafion®/mercury film coated GCE. Preconcentration potential:  $-0.9$  V (vs. Ag/AgCl); preconcentration time: 2 min. The SWASV was scanned from  $-1.0$  to  $-0.4$  V. SWASV parameters: modulation pulse height 50 mV, modulation frequency 200 Hz, effective scan rate  $800 \text{ mV s}^{-1}$ . Figures reproduced from reference [54]). Copyright 1999 Elsevier. C: The quantification of thallium in a cabbage sample using a standard addition method using deposition time of 10 mins; deposition potential of  $-0.9$  V; DTPA: 0.06 M where the dotted line is the original response, then the higher peaks correspond to 1.5 and 3 ng thallium. D: This shows the variation of the measured thallium current as a function of cadmium to thallium ratio. Lines represent a confidence interval of the measured signal of thallium [5 ng] in the absence of cadmium. Points represent a mean values ( $n \geq 2$ ) of the measured signal of thallium in the presence of different amounts of cadmium. Figures reproduced from reference ([59]). Copyright 2004 Polish Chemical Society.

thallium. The electrode was prepared by cleaning a GCE, then Nafion® is spin-coated onto the surface, after which, mercury was electro-deposited via applying a potential of  $-0.8$  V (vs. Ag/AgCl) for 4 min whilst being stirred. This electrode is then applied into the sensing of thallium. The Nafion® -mercury film electrode gave rise to a linear range of 244 pM–489 nM with a limit of detection (LoD) of 48 pM. The advantages are attributed to the ion-exchange properties of Nafion® [54]. This sensor was shown to detect thallium within spiked tap, rain and ground water (collected, filtered) which reported recoveries of

97–99 % [54]. Other work has reported the use of a mercury film modified GCE using EDTA and ascorbic acid for the sensing of thallium which reported a linear range of 1–500 nM with a LoD of 0.5 nM using a deposition potential and time of  $-1.4$  V (vs. SCE) and 600 s which was validated within spiked natural waters (no details of collection and pre-treatment are presented) [58].

Other approaches for the measurement of thallium (III) have reported the use of potentiometric stripping analysis using a poly(4-vinylpyridine) mercury film electrode [60]. Potentiometric stripping



analysis, also known as stripping chronopotentiometry, is where the thallium (III) is accumulated onto the electrode surface through being held at a suitable potential and time, after which, it is left in open circuit and oxidation of the metal from the electrode is effected by an oxidant diffusing to the electrode surface where the signal recorded is potential as a function of time. This approach reports the linear range of 4.9–489 nM with a LoD of 313 pM which are shown to allow thallium (III) to be measured with spiked ground and lake waters (collected, filtered) [60] which compared to SWASV where they use a poly(4-vinylpyridine) mercury film electrode obtained similar linear range and a LoD [61]. Other work has followed the use of potentiometric stripping analysis measuring thallium down to a LoD of 2 nM which was validated within spiked river water (details of collection etc. are missing) [62].

Elegant work has explored the use of DPASV with a hanging mercury drop electrode (HMDE) for thallium within wastewater, horseradish and water and cabbage certified reference materials [59]. Using the chelating agent, diethylenetriaminepentaacetic acid (DTPA), which is shown within Fig. 2C, the analysis of thallium recorded within a cabbage certified reference material where the dotted line is the response of the thallium in the origin material, followed by the addition of 1.5 ng and 3 ng thallium [59]. Note the presence of the stripping peak before the thallium signal is the stripping of cadmium and without the use of DTPA, the amount of cadmium would engulf the signal of the thallium [59]. Also shown in Fig. 2D is the variation of the measured thallium current as a function of cadmium to thallium ratio where the lines represent a confidence interval of the signal of 5 ng of thallium in the absence of cadmium. The points represent a mean values ( $n \geq 2$ ) of the signal of thallium in the presence of different amounts of cadmium. In summary, the signal of thallium can be observed up to a ratio of 1:700 in the presence of cadmium. The authors demonstrated that their electroanalytical protocol is useful for the measurement of thallium within the cabbage and water certified reference material and that within sewage and horseradish's that contained thallium rather than spiking, taking these samples from a highly contaminated region within Poland. Of note, they collected their water samples which were filter and used UV irradiation to decompose organic matter, while for the horseradish's, they used acidic mixture and microwave decomposition under elevated pressures. The authors validated their approach with ICP-MS. Other work has explored the sensing of thallium in the presence of lead and copper reporting a linear range of 11–97 nM and a LoD of 9.7 nM using a HMDE which it is explored within soil samples [63]. The authors need to validate their method comparing the electroanalytical response towards an independent laboratory instrument. More recent work has used mercury nanodroplets that are immobilised upon a chitosan-modified carbon paste electrode (CPE) which displayed a linear range of 1–400 ng mL<sup>-1</sup> with a LoD of 0.2 ng mL<sup>-1</sup> using a deposition potential and time of –1.0 V (vs. Ag/AgCl) and 300 s via DPASV. [64] The authors reported that the detection of thallium in the presence of cadmium and lead resulted in 6.8 % and 5.2 % depression of the thallium signal but found that this is acceptable. The authors showed merits in their approach by the measurement of thallium spiked within tap, well and wastewater (collected, filter and adjusted to the optimal pH) and human hair and a certified reference material.

Lukaszewski et al. [65] report upon the proof-of-concept determination of thallium and cadmium using the addition of the surfactant 0.1 % of polyethylene glycol in the presence of 0.1 M EDTA using HDME with ASV. Note that the use of surfactant has the effect of partial or complete suppression of the stripping peak, change in the peak potential, change in the dependence of peak-height on the deposition potential but in some cases, the peak-height might increase instead of being suppressed. The author demonstrate that thallium can be measured at 10 nM in the presence of cadmium [65]. Ciszewski and Lukaszewski [66] have extended the use of electrochemical masking where they report the measurement of thallium in the presence of lead by using HDME with DPASV using 0.2 M EDTA with 0.01 M tetrabutylammonium chloride (TBAC). The authors demonstrated that they could measure 5 nM

thallium in the presence of 0.05 M lead where they show their approach has merits in the sensing of thallium content within lead salts. Lukaszewski and Zembrzusi [57] have used a flow-injection DPASV using a mercury film electrode where they used 0.15 M EDTA and 0.1 M ascorbic acid where they applied their approach to the measurement of thallium in soil between 100 and 350 µg/L. Soils samples are collected (0.5 g) and are transferred into a beaker of a Teflon bomb where 2.5 mL hydrofluoric acid and hydrochloric and nitric acids (3:1) are added. This is closed and dried at 135 °C for 3 h. The resulting solution are heated on a graphite heater until evaporated where 2 mL of hydrogen peroxide are added to decompose organic substances. Last, the residue is dissolved into 1 mL of hot hydrochloric acid where EDTA, ascorbic acid is added and the pH is adjusted [57]. The authors noted that they can only partially extract the thallium from the soils (21–74 %) indicating further work is needed [57]. While the use of mercury has merits in the sensing of thallium, due to its toxicity, future regulations and occupational health consideration have results in the development of new alternatives electrode materials; the next section considers the use of bismuth modified electrodes.

## 2.2. Bismuth modified electrodes

Bismuth modified electrodes have the advantages of being non-toxic, it has a relatively high hydrogen overpotential where the cathodic behaviour is comparable to mercury, displays low background currents and is renewable alleviating the use of mechanical maintenance (*i.e.* polishing) and is promising in allowing full automation of film preparation–calibration–measurement–electrode regeneration cycle [67–71]. The use of bismuth modified electrodes are fabricated by the simultaneous deposition of bismuth along with the target metal(s). The quantification of thallium in the presence of cadmium and lead represents a common problem in stripping voltammetry due to overlapping stripping signals. See for example Fig. 3A, which displays the stripping peaks of cadmium and thallium which are overlapping (Fig. 3Aii) when using mercury film electrodes, but this is resolved when a bismuth-film electrode (Fig. 3Ai) produces separated peaks and offers quantification of the thallium, cadmium and lead [68].

Other work have reported the use of a bismuth film supported upon a GCE where a linear range of 48 nM–4.8 µM with a LoD reported to be 4.8 nM. The authors measured thallium within spiked lithium carbonate, which is used as a medication to treat manic-depressive disorder (bipolar disorder) [73]. The use of a bismuth bulk annular band electrode, where bismuth is the polycrystalline electrode, achieved low linear range from 48 pM to 489 nM with a LoD of 4.8 pM using a deposition potential of –1.0 V and time of 60 s [74]. The authors explored interfering species, where they found that cadmium, lead, copper and indium ions cause problems and hence they utilised the complexation agent EDTA. Other metal ions, such as antimony, zinc, cobalt, iron and manganese did not interfere as long as their concentration is below 0.1 mM. The authors went on to show that the electroanalytical method could be used for the sensing of thallium within tap, river (collected, filter and pH changed) and certified reference waters where the response was satisfactory with recovery in the range of 84–99 % [74]; further work should explore their response against an independent laboratory instrument. Lee and co-workers [75] reported the use of gas condensation method to form bismuth nanopowder, 20–50 nm in diameter, which were studied towards the sensing of thallium using a deposition time and potential of 600 s and –1.2 V (vs. SCE) which gave a linear range of 4.8 nM–2.4 µM with a LoD of 146 pM. The use of this study is rather limited as there are no real samples used. Related to the work reported above using nanopowder, Lezi and co-workers [76] have studied the use of disposable screen-printed carbon electrodes where they explored incorporating into the ink, bismuth oxide, bismuth aluminate and bismuth zirconate, all at 2 % (w/w). The authors favoured the use of bismuth oxide and bismuth aluminate since these show reproducibility, but for the bismuth zirconate it was too high to be used; the authors showed that they can

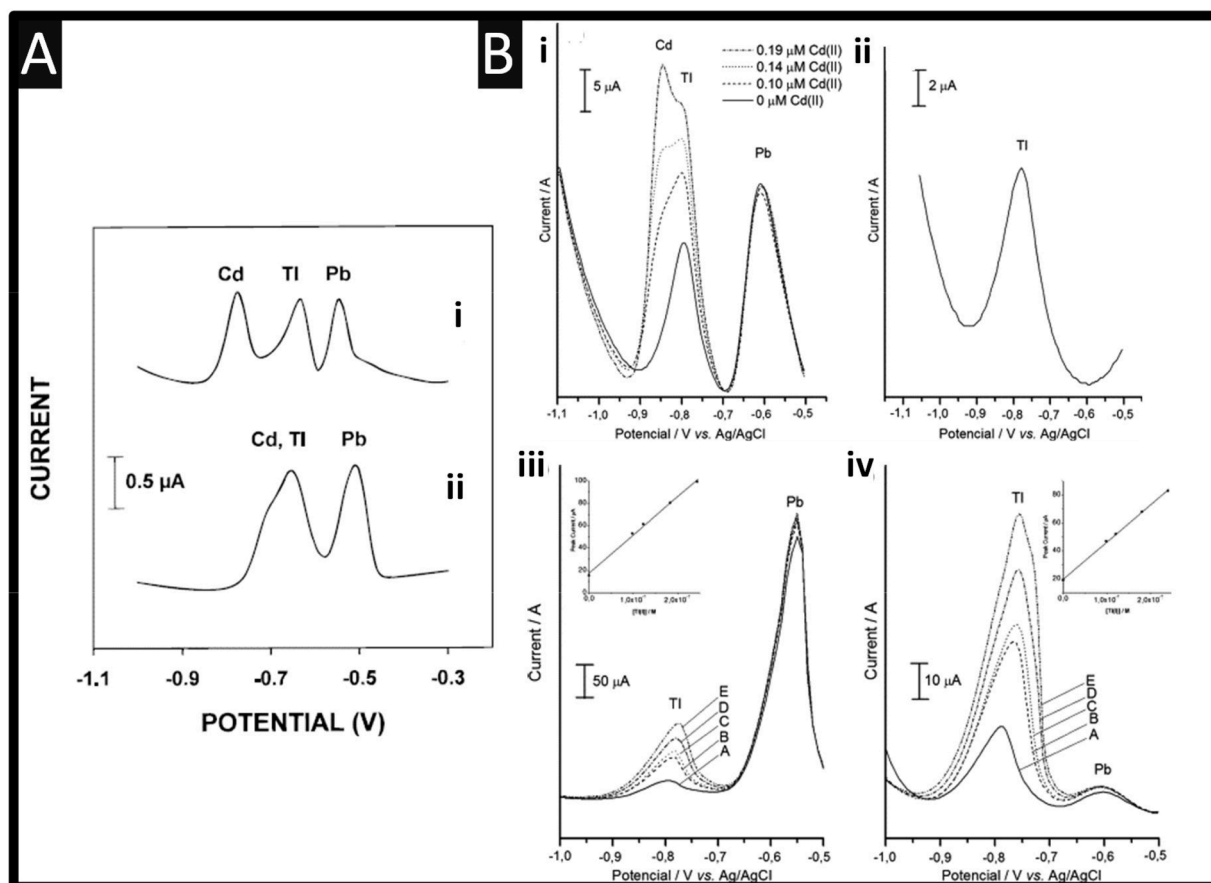


**Fig. 3.** A: Stripping voltammograms of a mixture of  $50 \mu\text{g L}^{-1}$  lead (II), cadmium (II), and thallium (I) at (i) bismuth and (ii) mercury thin-film electrodes. Solutions: 0.1 M acetate buffer (pH 4.5) containing  $1.9 \mu\text{M}$  bismuth (a) and  $49 \mu\text{M}$  mercury (b). Deposition for 120 s at  $-1.2 \text{ V}$  (vs. Ag/AgCl). Square-wave anodic voltammetric stripping scan with a frequency of 20 Hz, potential step of 5 mV, and amplitude of 25 mV. Figure reproduced from reference [68]. Copyright 2000 The American Chemical Society. B: Square-wave anodic voltammetric stripping  $0.1 \mu\text{M}$  thallium (i) +  $0.1 \mu\text{M}$  lead (II) at a bismuth film electrode BFE (i) in the absence (solid line) and presence (broken lines) of cadmium (II) (ii) in the presence of  $0.19 \mu\text{M}$  cadmium (II) +  $1.0 \text{ mM}$  EDTA. Deposition potential:  $-1.4 \text{ V}$  (vs. Ag/AgCl); time: 120 s;  $t_{\text{eq}}$ : 5 s; rotation speed: 240 rpm, square wave amplitude: 25 mV,  $\Delta E_s$ : 5 mV, square wave frequency: 20 Hz. Standard additions for (iii) river water and (iv) soil extract samples in acetate buffer. Curves: A, sample; B, C, D and E, sample + 9, 120, 180 and 240 nM, respectively, of thallium (I). Figure reproduced from reference [72]. Copyright 2007 Elsevier.

sense thallium within a certified lake water sample.

Caldeira et al. [77] studied the use of a bismuth film for the simultaneous detection of thallium, lead and zinc where a linear range of 0.5–120 nM is possible with a LoD of 2 nM using a deposition time of 120 second and a potential at  $-1.4 \text{ V}$  (vs. Ag/AgCl). They spiked thallium into a commercial juice showing a 105 % recovery with a relative standard deviation of 0.5 %. Work by Jorge and co-workers [72] have reported on the determination of thallium with rotating-disc bismuth film electrodes using a deposition potential and time of  $-1.4 \text{ V}$  (vs. Ag/AgCl and 120 seconds, respectively, which gave rise to a linear range of 12–150 nM with a LoD of 10.8 nM. The authors considered the interference of lead and cadmium ions upon the sensing of thallium, which as shown with Fig. 3Bi, one can see that the presence of cadmium (II) becomes problematic where the stripping peaks are overlapping. This is simply overcome though the addition of 1 mM EDTA, as shown within Fig. 3Bii, where the cadmium wave is absent allowing thallium to be quantified. [72] Note that the high amount of EDTA removes the cadmium peak completely, and those who have reported the use of a chelating agent to remove the interferences, should have added more concentration (see Fig. 2C). The authors went further by the determination of thallium within spiked river water (collected, filtered and adjusted the pH) and contaminated soil samples (collected, washed in water, filtered and then analysed) where, as shown within Fig. 3Biii and Biv, one can see the standard additions of thallium; the authors validated

the electroanalytical response by independent analysis by GF-AAS which has merits to be commercially adopted.

### 2.3. Antimony modified electrodes

Related to the use of bismuth modified electrodes, antimony modified electrodes have also been explored within stripping voltammetry [78]. The benefit of antimony modified electrodes have been summarised [79] which they exhibit favourably negative overvoltage of hydrogen evolution, wide operational potential window, convenient operation in acidic solutions of pH 2 or lower and a very small antimony stripping signal. However, its question as being a “green element”, such as that used to bismuth modified electrodes, with the answer being that its toxicity is lower than that of mercury, but it has its own toxicity. Antimony modified electrodes are operated in the same way as the bismuth modified electrode, where antimony ions are added into the metals ions which are simultaneously deposited. That said, there is evidence to suggest, for model analytes of cadmium and lead ions there is not a significant effect of applying a layer of antimony. [80] Sopha and co-workers have reported the use of an antimony film using a CPE for the simultaneous measurement of indium, thallium and zinc [81]. The authors showed that they can measure all the ions simultaneously but for this review, they report that a linear range of 48–489 nM with a LoD of 6.8 nM is possible for thallium, using a deposition potential and time of



–1.3 V (vs. Ag/AgCl) and 120 s respectively. That said, the method was not tested against interferences, noting that the presence of cadmium ions would interfere with the thallium signal, and it was not evaluated further within real/spiked samples. Other work has extended the above through the use of a GCE modified antimony film electrode for the simultaneous of indium and thallium [82]. The author used a deposition potential of –1.4 V (vs. Ag/AgCl) and a time of 120 s, where they report a linear range of 97–489 nM and LoD of 9.7 nM. Using a fixed concentration of 293 nM of thallium, the authors explored the presence of 200-times higher concentration of sodium, potassium and 3-times higher with calcium and a 33-times higher concentration of chloride, 30-times of magnesium and 20-times of manganese, all of which had no response on the thallium signal. The authors used EDTA to complex the ions of lead, cadmium and copper. Last, the authors explored the electroanalytical measurement of thallium within spiked river and tap water (collected and used as is), reporting recoveries of 89–105 % [82]. As it currently stands, the use of antimony film electrodes for the sensing of thallium are rather limited and as yet, they need independent validation against laboratory instruments. Last, the simultaneous determination of thallium and indium using two screen-printed carbon nanofiber-modified electrodes which are wired together, where one has immobilized 4-carboxybenzo-18-crown-6 while the other an *ex-situ* antimony film using multivariate calibration studies with partial least squares [83]. This sensor allowed thallium to be measured over the range of 47–976 nM using a deposition potential of –1.4 V (vs. Ag/AgCl) and a (stirred) time of 120 s. The authors demonstrated that their sensor can be used to measure spiked thallium within tap water (sample preparation details are absent) which was validated with independently laboratory instrument ICP-MS.

#### 2.4. Multi-walled carbon nanotubes

Multi-walled carbon nanotubes (MWCNTs) are multiple carbon nanotubes nested within one another. The diameter of the MWCNTs range from a few to tens of nanometres and the lengths are generally of the order of micrometres [84,85]. The advantages of using MWCNTs are that they have unique structural, mechanical and electronic properties but there is the disadvantages of the issue of metal impurities and nanographite impurities, but predominantly, the use of MWCNTs is that these can be easily modified with compounds. There are many reports of them being used effectively for the basis of sensing thallium [86–91]. MWCNTs have been modified with 3-Amino-1,2,4-triazole-5-thiol, which when coupled with differential pulse anodic stripping voltammetry (DPASV), gave a linear range of 48–489 nM towards thallium with a LoD of 6.3 nM. This sensor was prepared by chemically oxidising the MWCNTs via reflux within acidic solution for 2 h which were consequently modified with 3-Amino-1,2,4-triazole-5-thiol through using 4-Dimethylaminopyridine and *N,N'*-Dicyclohexylcarbodiimide dissolved into DMF, and stirring for 24 h at 100 °C; see Fig. 4A. These modified MWCNTs are then incorporated into a sensor, as summarised within Fig. 4B, where in summary, an indium tin oxide coated glass substrate was coated with the modified MWCNTs through dispersion for 2 h in DMF, where Triton X-100 and ethylene glycol are added. The suspension is then drop-casted onto the ITO surface using shadow masking and dried over hot plate at 200 °C for 2 h. The sensors performance is attributed to the incorporated thiol groups which are highly selective towards thallium ions and the useful electron transfer properties and high surface area of MWCNTs. This sensor was demonstrated to be useful for sensing thallium within spiked industrial waters which simply required that the sample is filter through a 0.45 micrometre filter and the pH is adjusted to the optimum value (pH 5), where recoveries

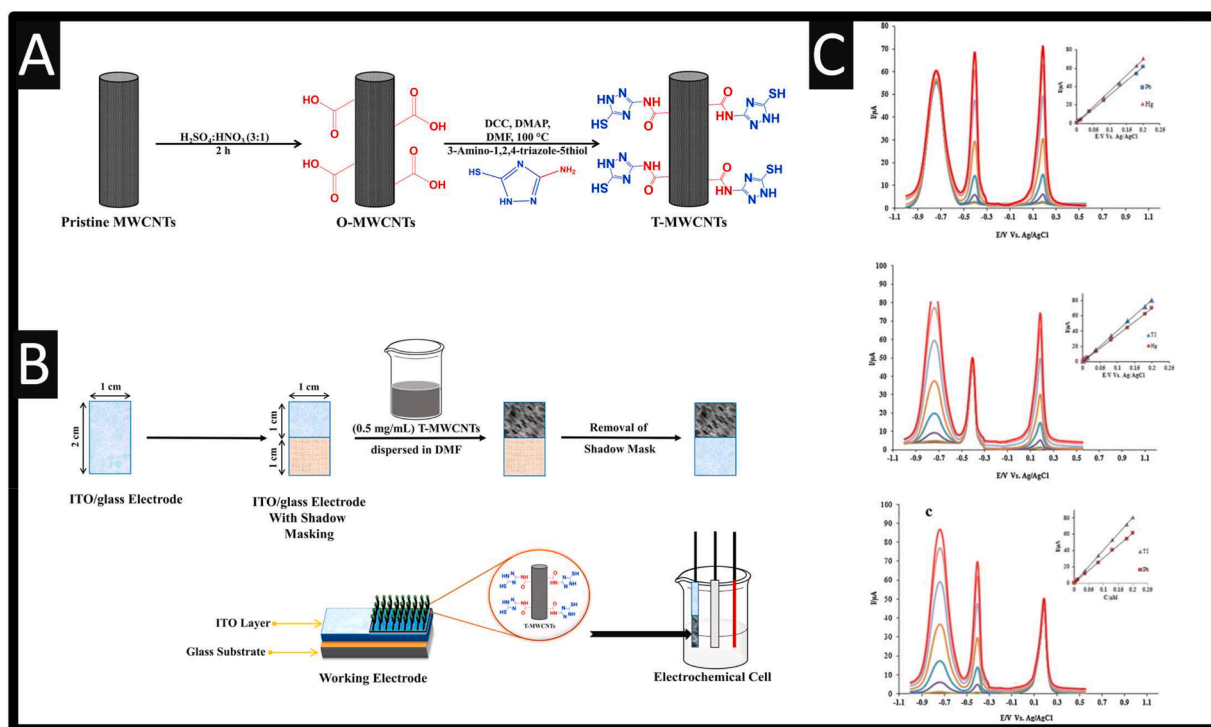


**Fig. 4.** A: An overview of the chemical oxidation and functionalization of pristine MWCNTs.; B: Also shown in the fabrication of MWCNTs – indium tin oxide (ITO) electrode. Figure reproduced from reference [86]. Copyright 2021 Elsevier. C: An overview of the square-wave voltammograms using OPFP-L<sub>2</sub>-graphene (top panel) towards the sensing of lead and mercury in the presence of a constant concentration of thallium. Inset shows calibration plot of the corrected electrochemical peak currents as a function of lead and mercury concentrations. The middle panel shows the addition of thallium and mercury in the presence constant concentration of lead and inset shows calibration plot of the corrected electrochemical peak currents as a function of thallium and mercury concentrations. The bottom panel shows the response of thallium and lead in the presence constant concentration of mercury where the insert shows the calibration plot of the corrected electrochemical peak currents as a function of thallium and lead concentrations. Figure reproduced from reference [92]. Copyright 2015 Elsevier.

over the range of 96.9–98.1 % are reported [86]. It may have been useful to compare their sensors approach with independent ICP-MS.

Nasiri-Majd and co-workers [88] have utilised MWCNTs which supported an imprinted nanosized polymer for the sensing of thallium. The polymer was prepared by bulk polymerisation using ethylene glycol dimethacrylate (crosslinking monomer) and methacrylic acid (functional monomer) in the presence of 2,2'-azobis(isobutyronitrile) (initiator). The polymer is then constructed into a CPE where the polymer, graphite and MWCNTs are mixed with silicon oil. This was evaluated towards the measurement of thallium which provided a linear range 14 nM–1.1  $\mu$ M with a LoD of 3.7 pM. Interferent tests were performed which indicated the imprinted nanosized polymer gave a selective response. The authors then demonstrated that thallium can be measured within spiked tap, well and wastewater and spiked human hair. In terms of the water samples, these are filtered and the pH is modified, while in the case of human hair, it is placed into acetone for 30 min, washed and dried. This is then digested by a mixture of nitric and perchloric acid, after which, it is diluted, pH is adjusted, and it is ready to be measured. The authors state that their sensor has a rapid response, it is simple to operate gives precise results at a low cost [88]. Jin and co-workers have reported upon the use of  $\text{MnO}_2/\text{Fe}_3\text{O}_4$  – sepiolite – MWCNTs which were fabricated via a hydrothermal method [93]. This composite has been reported to measure thallium over the range 489 pM–7.3  $\mu$ M with a LoD of 146 pM. Ultimately the authors demonstrated that this composite gave rise to the largest square wave anodic stripping voltammetry (SWASV) peak for thallium due to the larger electrode surface and the beneficial electron transfer [93]. In their evaluation of the selectivity of the sensor, they studied the effect of bismuth, lead, arsenic, nickel and indium ions while measuring 293 nM of thallium. They found that every ion affected the signal but less than 10 %, while the two interferences of cadmium and copper ions result in a measurement error of greater than 10 % [93], but the authors fail to state what interferences concentrations they used. That said, the author measured spiked thallium within tap, pool and well water (simply collected and changed to the optimal pH) also soil (dissolved into concentrated nitric acid, evaporated to dryness and the residue it is dissolved in water with the pH adjusted), which they compared their sensor with ICP-OES with good agreement.

The most impressive approach using MWCNTs has been reported by Mnyipika and Nomngongo [87] who have modified the MWCNTs with tin oxide nanoparticles via a hydrothermal process. They used this platform for the simultaneous determination of trace thallium and mercury alongside SWASV, utilising a deposition potential of  $-1.2$  V with a time of 120 s, which obtained a linear range of 14 pM–2.2  $\mu$ M towards thallium with a LoD of 4.4 pM. The authors studied the effect of cadmium ions as this is the major interference where they observed that up to 3.5  $\mu$ M of cadmium ions, there are no interference, but at 4.4  $\mu$ M the peaks overlap where a suitable chelating agent needs to be used. Last, they showed that the sensor can be used for the simultaneous determination of mercury and thallium in spiked river water (collected, filtered and pH adjusted) and compared the result with ICP-MS which gave a good agreement between both approaches. Using the combination of MWCNTs along with a bismuth film, supported upon a screen-printed carbon electrode (SPCE) has been reported, which gave a linear range of 0.01–1  $\mu$ M with a LoD of 2.8 nM. This sensor was then applied to the determination of thallium in spiked river water (no mention of how they prepared their sample) [91]. Other work has reported upon the simultaneous determination of thallium and lead using bismuth nanoparticles supported upon polydopamine functionalized MWCNTs [90], giving similar responses to that obtained by  $\text{SnO}_2$  - MWCNTs [87] but this is let down without the comparison to a laboratory standard (e.g. ICP-MS).

## 2.5. Graphene

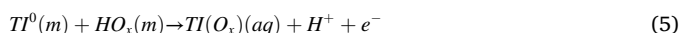
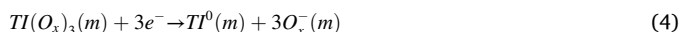
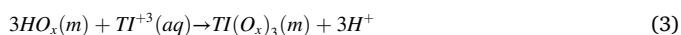
Graphene is an allotrope of carbon which is a one-atom-thick planar sheet of  $\text{sp}^2$  bonded carbon atoms in a honeycomb crystal lattice.

Graphene has reported outstanding material, physical, chemical with beneficial electrochemical properties including fast electron transfer, high conductivity, it is flexible and has a high surface area which can be functionalised by both non-covalent and covalent means [94–96]. It is surprising that when searching for the use of graphene for sensing thallium, there are very limited reports [92,97]. Using graphene deposited upon a GCE, the determination of thallium was reported within flour and grain products [97]. The graphene was formed via the electrochemical reduction of graphene oxide. Using DPASV alongside a deposition potential and time of  $-1.2$  V and 600 s, they are able to measure thallium over the range of 9.78–97.8 nM with a LoD of 6 nM. This was applied to the sensing of thallium within flour and grain products where the samples are dried in an oven for 55  $^\circ\text{C}$  for 24 h and then pulverized to a grain size of less than 0.06 mm. The samples are then placed into a Teflon beaker which are digested by adding 65 % nitric and 30 % hydrogen peroxide, followed by heating for 3 h. This is filtered where ascorbic acid and EDTA solutions are added and then adjusting to a pH of 4.5. The cereal products are shown to be over the range of 0.0268 to 0.0798 mg/kg, which is lower than the European maximum thallium level of  $0.46 (\pm 2.24)$  mg/kg, but it would have been useful if they compare their results against a laboratory standard.

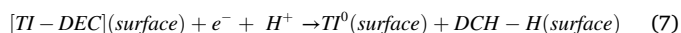
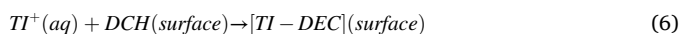
The use of graphene has been reported for the basis of a composite electrode using graphene, 1-n-octylpyridinium hexafluorophosphate and  $[2,4\text{-Cl}_2\text{C}_6\text{H}_3\text{C}(\text{O})\text{CHPhPh}_3]$ , a new synthetic phosphorus ylide, for the simultaneous detection of thallium, lead and mercury [92]. This approach uses the ylide,  $[2,4\text{-Cl}_2\text{C}_6\text{H}_3\text{C}(\text{O})\text{CHPhPh}_3]$ , for complexation of the target analytes. Using SWASV with a  $-1.1$  V deposition potential and time of 90 s this produced a linear range of 1.25–200 nM with a LoD of 0.35 nM. As shown within Fig. 4C, a summary of the square-wave voltammetry towards the simultaneous sensing of thallium, mercury and lead where the peaks are resolved. In studying the effects of interferences, adding in successive addition of cadmium into a solution with a fixed concentration of thallium, lead and mercury no interference was seen with thallium up to 15  $\mu$ M but over 18  $\mu$ M the peaks overlap. The authors also studied the interference of  $\text{Cu}^{2+}$ ,  $\text{Zn}^{2+}$ ,  $\text{K}^+$ ,  $\text{Na}^+$ ,  $\text{Ca}^{2+}$ ,  $\text{Mg}^{2+}$ ,  $\text{Al}^{3+}$ ,  $\text{Ni}^{2+}$ ,  $\text{Mn}^{2+}$ ,  $\text{Co}^{2+}$ ,  $\text{Cr}^{3+}$ ,  $\text{In}^{3+}$ ,  $\text{Ba}^{2+}$ ,  $\text{NH}_4^+$ ,  $\text{Cl}^-$ ,  $\text{NO}_3^-$ ,  $\text{SO}_4^{2-}$ ,  $\text{PO}_4^{3-}$  and  $\text{Fe}^{3+}$  up to 35  $\mu$ M they had no effect [92]. This sensor was shown to be successful for the measurement of spiked thallium, lead and mercury within tap, river water and soil samples (details are missing of how these were treated) which are compared with those obtained by GF-AAS. The agreement in results indicates that their sensor could replace GF-AAS in complex matrices, avoiding the use of expensive equipment providing a routine electroanalytical application [92]. One might suggest that there is scope for researcher to explore graphene for the sensing of thallium, but given the above results, there is not much value.

## 2.6. Other modifications

We now consider the various electrode surface modifications that do not fit into the above headings, these include silver nanoparticles [98], iridium oxide [99], glycine [100], an anion exchanger [101] and Prussian blue [102] modified electrodes. Modest responses to the measurement of thallium have been reported through to the use of Langmuir–Blodgett films of *p*-allylcalix[4]arene [103] and *p*-tert-butylcalix[4]arene [104], where the latter approach gave a linear range of 30 nM–4  $\mu$ M with a LoD of 20 nM which was applied into the sensing of thallium in tap and lake waters. 8-Hydroxyquinoline ( $\text{HO}_2$ ) has been used for the sensing of thallium (I) [105] and thallium (III) [106] using modified CPEs. In the sensing of thallium (III), it is accumulated in an open circuit using a stirred solution of pH 4.6 (Eq. (3)) and a modified 8-Hydroxyquinoline CPE [106]. Next the thallium (III) is electrochemically reduced to thallium metal (Eq. (4)) within a pH of 10 through using a deposition potential of  $-1.2$  V (vs.  $\text{Ag}/\text{AgCl}$ ) and a time of 2 mins, after which the potential is swept from negative to positive giving rise to the stripping peak, (Eq. (5)) which is summarised as: [106]



This approach reported a linear range of 0.5 nM–16 µM with a LoD of 0.23 nM. The authors studied the effect of interferences where no interference were observed from 1 mM of potassium and sodium ions and 10 µM of aluminium, silver, beryllium, chromium, cadmium, mercury, iron, nickel, lead, antimony, zinc, magnesium ions. That said, in using copper and bismuth these resulted in 53 and 84 % depressions of the thallium peak leading the author resort to using a chelating agent. The authors demonstrated the merit of the sensor in the measurement of thallium (III) in a US EPA water pollution quality control sample but as it didn't have any thallium, they spiked and demonstrated that they can measure within spiked sea water and human urine. While the author report that their method is simple, selective and sensitive the method was developed for the determination of thallium (III) [106], future more work is required to extend the number of samples being analysed and be compared to an independent laboratory instrument. Interesting work has been reported using a bulk CPE modified with a crown ether (dicyclohexyl-18-crown-6) which obtained a linear range of 14–1.2 µM and a LoD of 4.2 µM using a deposition potential and time of –1.2 V (vs. Ag/AgCl) and 5 min respectively [107]. This approach is summarised within Eqs. (6)–(8), where the thallium ions have to enter the cavity of the crown ether (DCH; Eq. (6)), which is then electrochemically reduced (Eq. (7)). After which, the electrochemical stripping is described by Eq. (8):



The authors explored their sensor into the spiked sample comprising tap, well and wastewater (collected, filter and pH adjusted), human hair and a certified reference material. Other notable work reports the approach to produce gold and silver nanoparticles using lignin derivatives [108–110]. For example, Konował et al. [108] report the development of silver nanoparticles, 55 nm average size, using ligno-sulfonic acid derivative (sodium lignosulfonate LS839) which acts as the silver ion reducer and stabiliser. The author used 0.05 M EDTA which enables the determination of thallium in the presence of 1000-fold excess of lead and the use of ascorbic acid reduces the excess of iron (Fe (III) to Fe(II)). [108] Using DPASV they demonstrated the electrode modification can detect thallium over the range of 12.2 nM–0.11 µM with a LoD of 4.6 nM and shown that they can measure thallium within soil samples from Rupea (Romania). Other work of highlight, is Hashemi and co-workers [111] who report ZIF-67, a metal-organic framework (MOF), within a bulk modified CPE for the sensing of thallium, which gave a linear range of 0.1 nM–0.5 µM and a LoD of 0.01 nM. The ZIF-67 was fabricated by dissolving cobalt nitrate salt into methyl alcohol with 2-methylimidazole, which was stirred for 2 h at room temperature and produced a purple precipitate, which was cleaned and then was dried for 24 h at 85 °C. The authors studied the interference from the following ions: potassium, manganese, nickel, iron, copper, ammonium, magnesium, lithium, aluminium, chromium, sodium, zinc and mercury, showing that none of them interferes with their thallium measurement. The selectivity of this electroanalytical sensor is based upon the size-exclusion properties of the MOF and compatibility between the diameter of the ZIF-67 pore window of 3.4 Angstrom and the effective diameter of hydrated thallium ions (2.5 Angstrom) [111]. The authors demonstrated their sensor has merit in the measurement of spiked thallium into river water (collected, filtered, pH changed), which gave recoveries of 94.6–96.0 %, while human urine was also spiked

(collected, diluted 1:1 with nitric acid, heated, filtered and pH changed) which gave a recovery value of 96.0–97.0 %. The authors analysed thallium within hair, where they collected hair samples from barbers close to their university. The specimens are placed into acetone for 15 mins, after which they are washed with water and desiccated. Next the sample is placed into an acid mixture which is dried, and then diluted within water with the pH being then changed. They found that the hair gave rise to 1.5 ng/g of thallium which is independently verified with FAAS. Also, the authors collected contaminated soil samples which was placed into Teflon vessels where they added 73 % HF and heated for 2 h. Next, a mixture of acid with hydrogen peroxide was added in; after evaporating, the solid is dissolved within nitric acid where the pH was changed. The electroanalytical sensor quantified thallium within soil at 0.155 µg/g and was independently verified with FAAS which reported 0.156 µg/g; it is gratifying that the electroanalytical sensors agreed well with FAAS for both the hair and soil samples.

### 3. Conclusions

We have overviewed the use of electroanalytical sensors for the determination of thallium. This has been reported at mercury, bismuth, antimony, MWCNT, graphene and crown ether and MOFs modified electrodes. Noting that the U.S. Environmental Protection Agency maximum contaminant level for thallium in drinking water is 2 µg L<sup>-1</sup> (0.098 µM/98 nM), there are plenty electroanalytical based approaches that fit this criteria; please see Table 1. Note, that a successful electroanalytical based response reports one of the lowest LoD, has the right magnitude of the linear range, and plus, it is compared to laboratory standards and has been used successfully in the sensing of the target analyte within a real sample which is independently validated against laboratory instruments. That said, it is pleasing to observe that many authors have compared their electroanalytical sensing with laboratory standards, namely FAAS, AAS, GFAAS, and ICP-OES/MS, which helps to validate their approach. We also note the range of real samples that have been analysed, for example spiked tap, lake, river, ground waters as well as the use of contaminated samples such as hair, soil, cabbage, horse-radish's which have been analysed independently against laboratory instruments. Further research should be focussed on expanding the field trials of electroanalytical based sensors for thallium and comparing their results with independent laboratory instruments to give more evidence that electroanalytical based sensors for thallium should be commercialized.

### CRedit authorship contribution statement

**Robert D. Crapnell:** Writing – review & editing, Writing – original draft. **Craig E. Banks:** Writing – review & editing, Writing – original draft, Conceptualization.

### Declaration of competing interest

The authors declare that they have no known competing financial interests or personal relationships that could have appeared to influence the work reported in this paper.

### Data availability

No data was used for the research described in the article.

### References

- [1] F.A.J.L. James, R.V. Jones, W.D.M. Paton, Of 'Medals and Muddles' the context of the discovery of Thallium: William Crookes's early spectro-chemical work, *Notes Rec. R. Soc. Lond.* 39 (1) (1984) 65–90.
- [2] W.J. Bank, D.E. Pleasure, K. Suzuki, M. Nigro, R. Katz, T. Poisoning, *Arch. Neurol.* 26 (5) (1972) 456–464.



- [3] R.S. Hoffman, R. Hoffman, Thallium poisoning during pregnancy: a case report and comprehensive literature review, *J. Toxicol. Clin. Toxicol.* 38 (7) (2000) 767–775.
- [4] O. Grunfeld, G. Hinostroza, Thallium poisoning, *Arch. Intern. Med.* 114 (1) (1964) 132–138.
- [5] L.E. Davis, J.C. Standerfer, M. Kornfeld, D.M. Abercrombie, C. Butler, Acute thallium poisoning: toxicological and morphological studies of the nervous system, *Ann. Neurol.* 10 (1) (1981) 38–44. : Official Journal of the American Neurological Association and the Child Neurology Society.
- [6] L.B. Zavalii, S.S. Petrikov, A.Y. Simonova, M.M. Potokhveriya, F. Zaker, Y. N. Ostapenko, K.K. Ilyashenko, T.I. Dikaya, O.B. Shakhova, A.K. Evseev, Diagnosis and treatment of persons with acute thallium poisoning, *Toxicol. Rep.* 8 (2021) 277–281.
- [7] G. Genchi, A. Carocci, G. Lauria, M.S. Sinicropi, A. Catalano, Thallium use, toxicity, and detoxification therapy: an overview, *Appl. Sci.* 11 (18) (2021) 8322.
- [8] A. Lennartson, Toxic thallium, *Nat. Chem.* 7 (7) (2015) 610–610.
- [9] I. Rossetto, F. Franconi, A.R. Felthous, F. Carabellese, G. Rivellini, F. Carabellese, An unusual case of serial poisoning of family members, *J. Forensic Sci.* 66 (5) (2021) 2060–2066.
- [10] A. Ghaderi, N. Vahdati-Mashhadian, Z. Oghabian, V. Moradi, R. Afshari, O. Mehrpour, Thallium exists in opioid poisoned patients, *DARU J. Pharm. Sci.* 23 (2015) 1–4.
- [11] S. Galván-Arzate, A. Santamaría, Thallium toxicity, *Toxicol. Lett.* 99 (1) (1998) 1–13.
- [12] S. Li, W. Huang, Y. Duan, J. Xing, Y. Zhou, Human fatality due to thallium poisoning: autopsy, microscopy, and mass spectrometry assays, *J. Forensic Sci.* 60 (1) (2015) 247–251.
- [13] J. Mulkey, F. Oehme, A review of thallium toxicity, *Vet. Hum. Toxicol.* 35 (5) (1993) 445–453.
- [14] P. Cvjetko, I. Cvjetko, M. Pavlica, Thallium toxicity in humans, *Arh. Za Hig. Rada Toksikol.* 61 (1) (2010) 111–118.
- [15] T.R. Kemnic, M. Coleman, Thallium Toxicity, StatPearls Publishing, Treasure IslandFL, 2022.
- [16] C. Rickwood, M. King, P. Huntsman-Mapila, Assessing the fate and toxicity of thallium I and thallium III to three aquatic organisms, *Ecotoxicol. Environ. Saf.* 115 (2015) 300–308.
- [17] T. Yumoto, K. Tsukahara, H. Naito, A. Iida, A. Nakao, A successfully treated case of criminal thallium poisoning, *J. Clin. Diagn. Res. JCDR* 11 (4) (2017) Od01–od02.
- [18] B. Campanella, L. Colomabaioni, E. Benedetti, A. Di Ciaula, L. Ghezzi, M. Onor, M. D'Orazio, R. Giannecchini, R. Petrin, E. Bramanti, Toxicity of thallium at low doses: a review, *Int. J. Environ. Res. Public Health* 16 (23) (2019) 4732.
- [19] S. Reith, Toxicological Review of Thallium and Compounds, US Environmental Protection Agency, Washington, DC, 2009.
- [20] R.S. Vardanyan, V.J. Hruby, R.S. Vardanyan, V.J. Hruby, 34 - Antimycobacterial Drugs. Synthesis of Essential Drugs, Elsevier, Amsterdam, 2006, pp. 525–534.
- [21] C.A. Lee, A Passion for Poison: A true Crime Story Like No other, the Extraordinary Tale of the Schoolboy Teacup Poisoner, John Blake, 2021.
- [22] J.H. Trestrail, Poisoners Throughout History, Criminal Poisoning: Investigational Guide for Law Enforcement, Toxicologists, Forensic Scientists, and Attorneys (2007) 1–27.
- [23] R.C. Gupta, R.C. Gupta, Chapter 47 - Non-Anticoagulant Rodenticides. Veterinary Toxicology, 3rd Ed., Academic Press, 2018, pp. 613–626.
- [24] <https://www.bbc.co.uk/news/world-asia-65084566>.
- [25] K. Jindal, M. Chawla, B.S. Nandkishor, S. Kiran, Successfully treated accidental thallium poisoning, *J. Indian Acad. Clin. Med.* 23 (2022).
- [26] B. Karbowska, Presence of thallium in the environment: sources of contaminations, distribution and monitoring methods, *Environ. Monit. Assess.* 188 (11) (2016) 640.
- [27] N. Belzile, Y.W. Chen, Thallium in the environment: a critical review focused on natural waters, soils, sediments and airborne particles, *Appl. Geochem.* 84 (2017) 218–243.
- [28] M.M. Hassanien, W.I. Mortada, I.M. Kenawy, H. El-Daly, Solid phase extraction and preconcentration of trace gallium, indium, and thallium using new modified amino silica, *Appl. Spectrosc.* 71 (2) (2017) 288–299.
- [29] A.O. Bajaj, R. Parker, C. Farnsworth, C. Law, K.L. Johnson-Davis, Method validation of multi-element panel in whole blood by inductively coupled plasma mass spectrometry (ICP-MS), *J. Mass Spectrom. Adv. Clin. Lab.* 27 (2023) 33–39.
- [30] M.J. Ahmed, M.L. Mia, A new simple, highly sensitive and selective spectrofluorimetric method for the speciation of thallium at pico-trace levels in various complex matrices using N-(pyridin-2-yl)-quinoline-2-carboxamide, *RSC Adv.* 11 (51) (2021) 32312–32328.
- [31] N.R. Biata, K.M. Dimpe, J. Ramontja, N. Mketo, P.N. Nomngongo, Determination of thallium in water samples using inductively coupled plasma optical emission spectrometry (ICP-OES) after ultrasonic assisted-dispersive solid phase microextraction, *Microchem. J.* 137 (2018) 214–222.
- [32] L.A. Oliveira, J.L.O. Santos, L.S.G. Teixeira, Determination of thallium in water samples via solid sampling HR-CS GF AAS after preconcentration on chromatographic paper, *Talanta* 266 (2024) 124945.
- [33] A. Darroudi, Ultra-preconcentration technique for the determination of thallium (I) in water samples by a combination of thallium (I)-imprinted polymer and vortex-assisted liquid-liquid microextraction, *Microchem. J.* 179 (2022) 107527.
- [34] H. Fazeli-rad, M.A. Taher, Ligandless, ion pair-based and ultrasound assisted emulsification solidified floating organic drop microextraction for simultaneous preconcentration of ultra-trace amounts of gold and thallium and determination by GFAAS, *Talanta* 103 (2013) 375–383.
- [35] A.S. Gugushe, A. Mpupa, P.N. Nomngongo, Ultrasound-assisted magnetic solid phase extraction of lead and thallium in complex environmental samples using magnetic multi-walled carbon nanotubes/zeolite nanocomposite, *Microchem. J.* 149 (2019) 103960.
- [36] C. Jin Mei, S. Ainliah Alang Ahmad, A review on the determination heavy metals ions using calixarene-based electrochemical sensors, *Arab. J. Chem.* 14 (9) (2021) 103303.
- [37] Z. Lukaszewski, M. Jakubowska, W. Zembrzusi, The mobility of thallium from bottom soil of the silesian-cracowian zinc-lead ore deposit region (Poland), *J. Geochem. Explor.* 184 (2018) 11–16.
- [38] C. Ariño, C.E. Banks, A. Bobrowski, R.D. Crapnell, A. Economou, A. Królicka, C. Pérez-Ràfols, D. Souli, J. Wang, Electrochemical stripping analysis, *Nat. Rev. Methods Primers* 2 (1) (2022) 62.
- [39] D. Poškus, G. Agafonovas, Radiotracer study of thallium underpotential deposition on a polycrystalline gold electrode in alkaline solutions, *J. Electroanal. Chem.* 493 (1–2) (2000) 50–56.
- [40] Y. Bonfil, M. Brand, E. Kirowa-Eisner, Characteristics of subtractive anodic stripping voltammetry of lead, cadmium and thallium at silver-gold alloy electrodes, *Electroanalysis* 15 (17) (2003) 1369–1376.
- [41] G. Herzog, D.W.M. Arrigan, Determination of trace metals by underpotential deposition–stripping voltammetry at solid electrodes, *TrAC Trends Anal. Chem.* 24 (3) (2005) 208–217.
- [42] E. Herrero, L.J. Buller, H.D. Abruña, Underpotential deposition at single crystal surfaces of Au, Pt, Ag and other materials, *Chem. Rev.* 101 (7) (2001) 1897–1930.
- [43] F.W. Campbell, Y.G. Zhou, R.G. Compton, Thallium underpotential deposition on silver nanoparticles: size-dependent adsorption behaviour, *New J. Chem.* 34 (2) (2010) 187–189.
- [44] V. Daujotis, E. Gaidamuskas, Effect of anions on the underpotential deposition of thallium(I) on polycrystalline silver, *J. Electroanal. Chem.* 446 (1) (1998) 151–157.
- [45] Y.Z. Ussipbekova, G.A. Seilkhanova, C. Jeyabharathi, F. Scholz, A.P. Kurbatov, M. K. Nauryzbaev, A. Berezovskiy, Electrochemical deposition and dissolution of thallium from sulfate solutions, *Int. J. Anal. Chem.* 2015 (2015) 357514.
- [46] C.-m. Wang, L. Zhu, Investigations of thallium (I) underpotential deposition on the silver rotating disk electrode and its analytical application, *Chem. Res. Chin. Univ.* 17 (1) (2001) 102–107.
- [47] J.W.F. Robertson, D.J. Tiani, J.E. Pemberton, Underpotential deposition of thallium, lead, and cadmium at silver electrodes modified with self-assembled monolayers of (3-Mercaptopropyl)trimethoxysilane, *Langmuir* 23 (8) (2007) 4651–4661.
- [48] T.C. Girija, M.V. Sangaranarayanan, Underpotential deposition of Tl on Ag in the presence of bromide ions – Estimation of specific capacitance for design of electrochemical supercapacitors, *J. Appl. Electrochem.* 36 (5) (2006) 531–538.
- [49] S. Bharathi, V. Yegnamaran, G.P. Rao, Simultaneous underpotential deposition of lead and thallium on polycrystalline silver-III, *J. Appl. Electrochem.* 24 (10) (1994) 981–988.
- [50] A.M.A. El-Halim, K. Jüttner, W.J. Lorenz, The electrocatalytic influence of thallium and lead underpotential adsorbates at silver single-crystal surfaces on the reduction processes of quinone, persulphate and protons, *J. Electroanal. Chem. Interfacial Electrochem.* 106 (1980) 193–207.
- [51] T.R. Copeland, R.K. Skogerboe, Anodic stripping voltammetry, *Anal. Chem.* 46 (14) (1974) 1257A–1268A.
- [52] Y.H. Lee, C.C. Hu, G. Kreysa, K.I. Ota, R.F. Savinell, Mercury drop electrodes. Encyclopedia of Applied Electrochemistry, Springer New York, New York, NY, 2014, pp. 1233–1240.
- [53] C. Ariño, N. Serrano, J.M. Díaz-Cruz, M. Esteban, Voltammetric determination of metal ions beyond mercury electrodes. A review, *Anal. Chim. Acta* 990 (2017) 11–53.
- [54] T.H. Lu, H.Y. Yang, I.W. Sun, Square-wave anodic stripping voltammetric determination of thallium(I) at a Nafion/mercury film modified electrode, *Talanta* 49 (1) (1999) 59–68.
- [55] J.W. Dieker, W.E. van der Linden, G. den Boef, Amperometric complex-titrations at a dropping mercury electrode, employing normal pulse polarography, *Talanta* 24 (5) (1977) 321–322.
- [56] R.G. Dhaneshwar, L.R. Zarparkar, Simultaneous determination of thallium and lead at trace levels by anodic-stripping voltammetry, *Analyst* 105 (1249) (1980) 386–390.
- [57] Z. Lukaszewski, W. Zembrzusi, Determination of thallium in soils by flow-injection-differential pulse anodic stripping voltammetry, *Talanta* 39 (3) (1992) 221–227.
- [58] S.A. Kozina, Stripping voltammetry of thallium at a film mercury electrode, *J. Anal. Chem.* 58 (10) (2003) 954–958.
- [59] B. Krasnoděbska-Ostręga, E. Stryjewska, Voltammetric determination of thallium in water and plant material, *Chem. Analityczna* 49 (4) (2004) 519.
- [60] J.M. Zen, W.M. Wang, A.S. Kumar, Potentiometric stripping analysis of traces of thallium(III) at a Poly(4-Vinylpyridine)/mercury film electrode, *Electroanalysis* 13 (4) (2001) 321–324.
- [61] J.M. Zen, J.W. Wu, Square-wave voltammetric stripping analysis of thallium (III) at a poly (4-vinylpyridine)/mercury film electrode, *Electroanalysis* 9 (4) (1997) 302–306.
- [62] R. Cleven, L. Fokkert, Potentiometric stripping analysis of thallium in natural waters, *Anal. Chim. Acta* 289 (2) (1994) 215–221.
- [63] Y. Cruz-Hernández, M. Villalobos, J.L. González-Chavez, N. Martínez-Villegas, Optimizing the differential pulse anodic stripping voltammetry method with a hanging mercury electrode for thallium (I) determination in the presence of lead

- (II) and copper (II) for application in contaminated soils, *Rev. Int. Contam. Ambient.* 35 (2) (2019) 481–494.
- [64] S. Mohammadi, M.A. Taher, H. Beitollahi, Mercury nanodroplets immobilized on the surface of a chitosan-modified carbon paste electrode as a new thallium sensor in aqueous samples, *J. Electrochem. Soc.* 164 (9) (2017) B476.
  - [65] Z. Lukaszewski, M.K. Pawlak, A. Ciszewski, Determination of thallium and lead in cadmium salts by anodic stripping voltammetry with addition of surfactants to suppress the cadmium peaks, *Talanta* 27 (2) (1980) 181–185.
  - [66] A. Ciszewski, Z. Lukaszewski, Determination of thallium in lead salts by differential pulse anodic-stripping voltammetry, *Talanta* 30 (11) (1983) 873–875.
  - [67] R. Pauliukaitė, S.B. Hocevar, B. Ogorevc, J. Wang, Characterization and applications of a bismuth bulk electrode, *Electroanalysis* 16 (9) (2004) 719–723.
  - [68] J. Wang, J. Lu, S.B. Hocevar, P.A.M. Farias, B. Ogorevc, Bismuth-coated carbon electrodes for anodic stripping voltammetry, *Anal. Chem.* 72 (14) (2000) 3218–3222.
  - [69] J. Wang, Stripping analysis at bismuth electrodes: a review, *Electroanalysis* 17 (15–16) (2005) 1341–1346.
  - [70] A. Economou, Bismuth-film electrodes: recent developments and potentialities for electroanalysis, *TrAC Trends Anal. Chem.* 24 (4) (2005) 334–340.
  - [71] E.A. Hutton, B. Ogorevc, S.B. Hocevar, F. Weldon, M.R. Smyth, J. Wang, An introduction to bismuth film electrode for use in cathodic electrochemical detection, *Electrochem. Commun.* 3 (12) (2001) 707–711.
  - [72] E.O. Jorge, M.M.M. Neto, M.M. Rocha, A mercury-free electrochemical sensor for the determination of thallium(I) based on the rotating-disc bismuth film electrode, *Talanta* 72 (4) (2007) 1392–1399.
  - [73] V.A. Tarasova, Voltammetric determination of thallium(I) at a mechanically renewed Bi-graphite electrode, *J. Anal. Chem.* 62 (2) (2007) 157–160.
  - [74] K. Wegiel, K. Jedlińska, B. Baś, Application of bismuth bulk annular band electrode for determination of ultratrace concentrations of thallium(I) using stripping voltammetry, *J. Hazard. Mater.* 310 (2016) 199–206.
  - [75] G.-J. Lee, H.-M. Lee, Y.-R. Uhm, M.-K. Lee, C.-K. Rhee, Square-wave voltammetric determination of thallium using surface modified thick-film graphite electrode with Bi nanopowder, *Electrochem. Commun.* 10 (12) (2008) 1920–1923.
  - [76] N. Lezi, C. Kokkinos, A. Economou, M.I. Prodromidis, Voltammetric determination of trace Tl(I) at disposable screen-printed electrodes modified with bismuth precursor compounds, *Sens. Actuators B Chem.* 182 (2013) 718–724.
  - [77] A. Caldeira, C. Gouveia-Cardade, R. Pauliukaite, C.M.A. Brett, Application of square wave anodic stripping voltammetry for determination of traces of Tl(I) at carbon electrodes *in situ* modified with Bi films, *Electroanalysis* 23 (6) (2011) 1301–1305.
  - [78] S.B. Hocevar, I. Švancara, B. Ogorevc, K. Vytrās, Antimony film electrode for electrochemical stripping analysis, *Anal. Chem.* 79 (22) (2007) 8639–8643.
  - [79] N. Serrano, J.M. Díaz-Cruz, C. Ariño, M. Esteban, Antimony-based electrodes for analytical determinations, *TrAC Trends Anal. Chem.* 77 (2016) 203–213.
  - [80] C.W. Foster, A.P. de Souza, J.P. Metters, M. Bertotti, C.E. Banks, Metallic modified (bismuth, antimony, tin and combinations thereof) film carbon electrodes, *Analyst* 140 (22) (2015) 7598–7612.
  - [81] H. Sopha, L. Baldrianova, E. Tesarova, S.B. Hocevar, I. Svancara, B. Ogorevc, K. Vytrās, Insights into the simultaneous chronopotentiometric stripping measurement of indium(III), thallium(I) and zinc(II) in acidic medium at the *in situ* prepared antimony film carbon paste electrode, *Electrochim. Acta* 55 (27) (2010) 7929–7933.
  - [82] J. Zhang, Y. Shan, J. Ma, L. Xie, X. Du, Simultaneous determination of indium and thallium ions by anodic stripping voltammetry using antimony film electrode, *Sens. Lett.* 7 (4) (2009) 605–608.
  - [83] C. Pérez-Rafols, N. Serrano, J.M. Díaz-Cruz, C. Ariño, M. Esteban, Simultaneous determination of Tl(I) and In(III) using a voltammetric sensor array, *Sens. Actuators B Chem.* 245 (2017) 18–24.
  - [84] X. Ji, R.O. Kadara, J. Krussma, Q. Chen, C.E. Banks, Understanding the physicoelectrochemical properties of carbon nanotubes: current state of the art, *Electroanalysis* 22 (1) (2010) 7–19.
  - [85] A. Kaliyaraj Selva Kumar, Y. Lu, R.G. Compton, Voltammetry of carbon nanotubes and the limitations of particle-modified electrodes: are carbon nanotubes electrocatalytic? *J. Phys. Chem. Lett.* 13 (37) (2022) 8699–8710.
  - [86] A. Lochab, M. Saxena, K. Jindal, M. Tomar, V. Gupta, R. Saxena, Thiol-functionalized multiwall carbon nanotubes for electrochemical sensing of thallium, *Mater. Chem. Phys.* 259 (2021) 124068.
  - [87] S.H. Mnyipika, P.N. Nomngongo, Square wave anodic stripping voltammetry for simultaneous determination of trace Hg (III) and Tl (I) in surface water samples using SnO<sub>2</sub>@MWCNTs modified glassy carbon electrode, *Int. J. Electrochem. Sci.* 12 (6) (2017) 4811–4827.
  - [88] M. Nasiri-Majid, M.A. Taher, H. Fazlirad, Synthesis and application of nano-sized ionic imprinted polymer for the selective voltammetric determination of thallium, *Talanta* 144 (2015) 204–209.
  - [89] M. Ghanei-Motlagh, M. Baghayeri, Determination of trace Tl(I) by differential pulse anodic stripping voltammetry using a novel modified carbon paste electrode, *J. Electrochem. Soc.* 167 (6) (2020) 066508.
  - [90] M. Nodehi, M. Baghayeri, A. Kaffash, Application of BiNPs/MWCNTs-PDA/GC sensor to measurement of Tl (I) and Pb (II) using stripping voltammetry, *Chemosphere* 301 (2022) 134701.
  - [91] J. Kozak, K. Tyszczyk-Rotko, M. Rotko, Voltammetric screen-printed carbon sensor modified with multiwalled carbon nanotubes and bismuth film for trace analysis of thallium(I), *Physicochem. Probl. Miner. Process.* 55 (6) (2019) 1422–1428.
  - [92] H. Bagheri, A. Afkhami, H. Khoshafar, M. Rezaei, S.J. Sabounchei, M. Sarlakifar, Simultaneous electrochemical sensing of thallium, lead and mercury using a novel ionic liquid/graphene modified electrode, *Anal. Chim. Acta* 870 (2015) 56–66.
  - [93] X. Jin, M. Baghayeri, M. Nodehi, M.S. Koshki, A. Ramezani, M. Fayazi, Y. Xu, Z. Hua, Y. Lei, P. Makvandi, Evaluation of thallium ion as an effective ion in human health using an electrochemical sensor, *Environ. Res.* 238 (2023) 117026.
  - [94] D.A.C. Brownson, D.K. Kampouris, C.E. Banks, An overview of graphene in energy production and storage applications, *J. Power Sources* 196 (11) (2011) 4873–4885.
  - [95] E.P. Randviir, D.A.C. Brownson, C.E. Banks, A decade of graphene research: production, applications and outlook, *Mater. Today* 17 (9) (2014) 426–432.
  - [96] D.A.C. Brownson, D.K. Kampouris, C.E. Banks, Graphene electrochemistry: fundamental concepts through to prominent applications, *Chem. Soc. Rev.* 41 (21) (2012) 6944–6976.
  - [97] B. Karbowska, T. Rębiś, G. Milczarek, Electrode modified by reduced graphene oxide for monitoring of total thallium in grain products, *Int. J. Environ. Res. Public Health* 15 (4) (2018) 653.
  - [98] A. Modrzejewska-Sikorska, E. Konował, B. Karbowska, D. Szatkowska, New electrode material GCE/AgNPs-D3 as an electrochemical sensor used for the detection of thallium ions, *Electroanalysis* 35 (5) (2023) e202200281.
  - [99] J.A. Cox, B.K. Das, Voltammetric characterization and determination of thallium (III) at a glassy carbon electrode modified with a film containing iridium oxide, *Electroanalysis* 1 (1) (1989) 57–61.
  - [100] A. Shah, A. Nisar, K. Khan, J. Nisar, A. Niaz, M.N. Ashiq, M.S. Akhter, Amino acid functionalized glassy carbon electrode for the simultaneous detection of thallium and mercuric ions, *Electrochim. Acta* 321 (2019) 134658.
  - [101] W. Diewald, K. Kalcher, C. Neuhold, X. Cai, R.J. Magee, Voltammetric behaviour of thallium(III) on carbon paste electrodes chemically modified with an anion exchanger, *Anal. Chim. Acta* 273 (1) (1993) 237–244.
  - [102] J.M. Zen, P.Y. Chen, *Indian J. Chem.* 41A (2003) 839–842.
  - [103] H. Dong, H. Zheng, L. Lin, B. Ye, Determination of thallium and cadmium on a chemically modified electrode with Langmuir–Blodgett film of p-allylcalix[4] arene, *Sens. Actuators B Chem.* 115 (1) (2006) 303–308.
  - [104] L. Zou, Y. Zhang, H. Qin, B. Ye, Simultaneous DETERMINATION OF THALLIUM AND LEAD ON A CHEMICALLY MODIFIED ELECTRODE WITH LANGMUIR–BLODGETT FILM OF A p-tert-Butylcalix[4]arene Derivative, *Electroanalysis* 21 (23) (2009) 2563–2568.
  - [105] Q. Cai, S.B. Khoo, Differential pulse stripping voltammetric determination of thallium with an 8-hydroxyquinoline-modified carbon paste electrode, *Electroanalysis* 7 (4) (1995) 379–385.
  - [106] Q. Cai, S.B. Khoo, Determination of trace thallium after accumulation of thallium (III) at a 8-hydroxyquinoline-modified carbon paste electrode, *Analyst* 120 (4) (1995) 1047–1053.
  - [107] S. Cheraghi, M.A. Taher, H. Fazlirad, Voltammetric sensing of thallium at a carbon paste electrode modified with a crown ether, *Microchimica Acta* 180 (11) (2013) 1157–1163.
  - [108] E. Konował, A. Modrzejewska-Sikorska, A.M. Kopaczewska, B. Karbowska, New electrode material GCE/AgNPs-LS/Hg based on nanosilver produced with the use of biopolymers, *Electroanalysis* 33 (9) (2021) 2071–2077.
  - [109] A. Modrzejewska-Sikorska, E. Konował, K. Kosińska, B. Karbowska, Modyfikacja elektrody glassy carbon kompozytem na bazie nanocząstek koloidalnego srebra stabilizowanych pochodnymi sieciowanymi skrobi dla potrzeb woltamperometrycznego oznaczania talu, *Przem. Chem.* 102 (2023).
  - [110] B. Karbowska, T. Rębiś, G. Milczarek, Mercury-modified lignosulfonate-stabilized gold nanoparticles as an alternative material for anodic stripping voltammetry of thallium, *Electroanalysis* 29 (9) (2017) 2090–2097.
  - [111] F. Hashemi, A.R. Zanganeh, F. Naeimi, M. Tayebani, Construction of a Tl(I) voltammetric sensor based on ZIF-67 nanocrystals: optimization of operational conditions via response surface design, *Anal. Bioanal. Chem.* 413 (20) (2021) 5215–5226.
  - [112] A.R. Curtis, Determination of trace amounts of thallium in urine, using the mercury-film electrode and differential pulse anodic stripping voltammetry, *J. Assoc. Off. Anal. Chem.* 57 (6) (2020) 1366–1372.
  - [113] L.K. Hoeflich, R.J. Gale, M.L. Good, Differential pulse polarography and differential pulse anodic stripping voltammetry for determination of trace levels of thallium, *Anal. Chem.* 55 (9) (1983) 1591–1595.
  - [114] K. Mutsuo, N. Tomohiko, Use of a hanging mercury drop electrode in the alternating current polarographic analysis of thallium(I), *Bull. Chem. Soc. Jpn.* 41 (10) (1968) 2401–2405.
  - [115] C. von Laar, R. Reinke, J. Simon, Determination of thallium in soils by differential pulse anodic stripping voltammetry by means of a mercury film electrode, *Fresenius, J. Anal. Chem.* 349 (8) (1994) 692–693.
  - [116] K. Domańska, K. Tyszczyk-Rotko, Integrated three-electrode screen-printed sensor modified with bismuth film for voltammetric determination of thallium(I) at the ultratrace level, *Anal. Chim. Acta* 1036 (2018) 16–25.
  - [117] N. Spano, A. Panzanelli, P.C. Piu, M.I. Pilo, G. Sanna, R. Seeber, A. Tapparo, Anodic stripping voltammetric determination of traces and ultratraces of thallium at a graphite microelectrode: method development and application to environmental waters, *Anal. Chim. Acta* 553 (1) (2005) 201–207.